PUBLICATIONS OF THE ASTRONOMICAL SOCIETY OF THE PACIFIC, **119**: 605–615, 2007 June
© 2007. The Astronomical Society of the Pacific. All rights reserved. Printed in U.S.A.

Measuring the Balmer Jump and the Effective Gravity in FGK Stars

MICHAEL S. BESSELL

Research School of Astronomy and Astrophysics, Australian National University, Mount Stromlo, Weston, Australia; bessell@mso.anu.edu.au

Received 2006 October 17; accepted 2007 May 18; published 2007 June 21

ABSTRACT. It is difficult to accurately measure the effective gravity ($\log g$) in late-type stars using broadband (e.g., *UBV* or SDSS) or intermediate-band (*uvby*) photometric systems, especially when the stars can cover a range of metallicities and reddenings. However, simple spectroscopic observational and data reduction techniques can yield accurate values for $\log g$ through comparison of the Balmer jumps of low-resolution spectra with recent grids of synthetic flux spectra.

Online material: color figure

1. INTRODUCTION

The abundance analyses of the oldest stars in the Galaxy are of great importance to our understanding of which elements were created during the life and death of the first generation of stars and how the fraction of heavy elements built up through the evolution of subsequent generations of stars. The effective temperature is the most important stellar atmosphere parameter to assign in the determination of abundances, but for those elements only represented by lines of the neutral species, it is necessary to establish the electron pressure or the effective gravity of the star. This is because hotter than about 4500 K, most of the heavy elements are once ionized, and significant corrections are required to determine the total element abundances from the neutral species. Theoretical isochrones for a range of metallicities and ages are readily available (Pietrinferni et al. 2006; VandenBerg 2000; Salasnich et al. 2000), and the normal $\log (L/L_\odot)$ versus $\log T_{\rm eff}$ relations can be readily transformed to $\log g$ versus $T_{\rm eff}$ [$\log g = 4 \log T_{\rm eff} - \log (L/L_\odot) - 10.608$].

Figure 1 shows a typical halo isochrone for an age of 12 Gyr. For old stars (age > 10 Gyr), the shape of the isochrone changes little as the main-sequence turnoff (TO) moves to cooler temperatures with older age. As can be seen from the figure, for a given temperature, there are normally only three different possible values for $\log g$ for a halo star, depending on whether the star is on the main sequence (MS), the subgiant/giant branch (SGB), or on the horizontal branch (HB) or asymptotic giant branch (AGB). Cooler than about 5500 K, it is generally quite easy to choose between a MS ($\log g = 5$), GB ($\log g = 3.5$), and HB star ($\log g = 2.5$), but near the MS turnoff, the differences in gravity are quite small and more difficult to discern.

The Balmer discontinuity is an obvious feature to measure in the spectra of late-type halo stars in order to determine $\log g$. Blueward of 3636 Å, the continuous opacity is mainly H^-, whereas redward it is H^- plus H I. As $\log g$ (and $\log P_e$) decreases, the H^- opacity decreases and the size of the Balmer discontinuity increases. But as the H I opacity decreases steeply with decreasing temperature, the Balmer jump becomes less sensitive to changes in $\log g$.

Although low-dispersion spectra are regularly taken of halo stars in order to measure the H and K lines of Ca II and the Hδ line for metallicity and temperature estimates, little or no effort is put into measuring the Balmer discontinuity. I think that there are three main reasons for this. First, as the Balmer discontinuity is near the confluence of the hydrogen lines, the continuum is changing rapidly and it seems impossible to unequivocally extrapolate a curved line that fits the continuum from the 4100 to 4800 Å region, where the continuum is well defined. Second, the sensitivity of most spectrographs and CCDs decreases rapidly below 3900 Å, leading many people to think there is little point in observing below 3600 Å. And finally, many think that it may be possible to overcome these difficulties only if a full relative-absolute spectrophotometric calibration is undertaken, and this seems like too much effort for an uncertain return.

This paper aims to show how, with a minimal amount of extra effort at both the telescope and with the data reduction, the Balmer jump can be readily measured and compared with similar data from the detailed grid of synthetic spectra provided by Munari et al. (2005).

2. TECHNIQUES

2.1. Atmospheric Dispersion

When doing ground-based spectroscopy in the UV/blue, it is highly desirable that the effect of atmospheric dispersion is minimized, either by using an atmospheric dispersion corrector (Filippenko 1982) or by rotating the spectrograph slit so that it is parallel to the atmospheric dispersion. Otherwise, at large zenith distances, if the guider is centering the green or red image, a significant proportion of the UV/blue light will miss

the slit. But, as the Balmer jump is measured at one wavelength, it is not absolutely essential to measure the same proportion of light at all wavelengths. However, although a reasonable discontinuity may be measured under these circumstances, any possibility of measuring a temperature-sensitive slope or color, such as $B - V$, is lost. If an atmospheric dispersion corrector is unavailable, spectra should be taken with the slit tracking the parallactic angle, or the star should be acquired in that mode and then observed with the position angle fixed to use an offset guide star in an alt-az telescope.

2.2. Division by Blackbody Spectrum

Bessell (1999) discusses the advantages of observing smooth-spectrum stars as part of any observing program. After the raw spectra have been extracted, the first step is to divide all spectra by the normalized spectrum of a star with a near-blackbody (BB) energy distribution.

There are several near-continuous bright white dwarfs (WDs) that are well suited for such division. These are EG 131 and L745−46a, which are accessible in opposite seasons, together with vMa 2 and two carbon-rich white dwarfs, LHS 43 (Bessell 1999) and LHS 4043 (Dufour et al. 2005). It is necessary to remove the weak C_2 bands from the carbon WDs and the Ca II H and K and Mg I lines from L745−46a and vMa 2, or fit a line through the continuum before division. Greenstein & Liebert (1990) and Bergeron et al. (2001) discuss the spectra of these stars, while Koester & Wolff (2000) and Dufour et al. (2005) discuss the theoretical fluxes of some of the stars.

There are two main reasons for dividing by a normalized near-BB spectrum. First, in the red it removes most of the atmospheric (telluric) absorption lines, and second, for both blue and red spectra, it removes most of the instrumental response due to vignetting, grating blaze, filters, mirrors, and CCD response. The net effect of this division is to provide spectra in which the continuum level changes slowly and smoothly with wavelength, which in turn means the corrections (with wavelength) to place the fluxes on a relative absolute flux scale can be well fitted with a smooth low-order polynomial or spline.

2.3. Linearization of the Continuum

An unanticipated dividend of the division by a warm near-BB spectrum was the fact that the continuum levels of FGK stars above and below the Balmer jump were transformed from curves into almost straight lines. This enables the continua to be extrapolated with confidence to 3636 Å, and the Balmer jump to be measured accurately and consistently.

Division by EG 131, with a blackbody temperature of about 11,800 K, straightens the continuum in stars with temperatures from 7500 to 5000 K. Division by the cooler L745−46a (≈8600 K) leaves some residual curvature for spectra hotter than 6500 K, but is good for cooler stars. The two carbon-rich white dwarfs LHS 43 and LHS 4043 have intermediate blackbody temperatures between EG 131 and L745−46a; vMa 2 is cooler.

Figure 2 shows examples of raw extracted blue spectra obtained with the Double Beam Spectrograph (DBS) on the Australian National University 2.3 m telescope. The data have not been flat fielded. From the top are the white dwarf LHS 43 and the halo stars G64−12 (sdF0; 6500 K, $\log g = 4.0$, [Fe/H] $= -3.4$), HD 84937 (sdF5; 6200 K/4.0/−2.3), G24−3 (sdF8; 5900 K/4.2/−1.7), and CD −38 245 (4800 K/1.5/−4.1). The bracketed quantities are the approximate stellar parameters of the stars. The spectra are offset by 0.2 divisions for clarity.

Figure 3 shows the same raw spectra divided by the spectrum of EG 131. The weak carbon bands in LHS 43 and the Balmer jumps in the halo stars are much more obvious and easier to measure in the divided spectra.

3. THEORETICAL FLUXES: MODEL SYNTHETIC SPECTRA

Line-blanketed fluxes are available for the ATLAS9 and MARCS grid of model atmospheres. The Munari et al. (2005) ATLAS9 synthetic spectra at 1 Å resolution are particularly useful. The MARCS[1] sampled photospheric fluxes, available on their Web site, are provided with a warning that they are not likely to give a good representation of the integrated fluxes in a limited wavelength region. However, they look adequate for the lowest metallicities.

Figure 4 shows Munari et al. synthetic f_λ spectra for an abundance of [Fe/H] $= -2.5$, a temperature of 5750 K, and three different effective gravities. The spectra have been smoothed to a resolution of 3 Å, the same as the DBS data. The Balmer discontinuity at 3636 Å can be seen, but the slope of the continuum redward of this limit makes it difficult to measure it.

The synthetic spectra can also be divided by an 11,800 K blackbody to measure the theoretical Balmer jumps more reliably. Figure 5 gives the same 5750 K spectra divided by an 11,800 K blackbody. Figures 6 to 10 show similarly divided Munari et al. synthetic spectra for several more temperatures and sets of gravities appropriate for main-sequence, giant-branch, and horizontal or asymptotic giant branch stars. For each temperature plot, the divided spectra have been normalized at 5300 Å and are plotted with equal offsets for better visibility. One can draw straight lines through the continua on the various figures to see how linear the continua of the divided observed and synthetic spectra are and how well defined the Balmer jumps are, even when they are small.

4. BALMER JUMP MEASUREMENTS

4.1. Theoretical Spectra

The tabulated model spectra were interpolated to a uniformly spaced wavelength scale (using the task *scrunch*) and then

[1] See http://marcs.astro.uu.se.

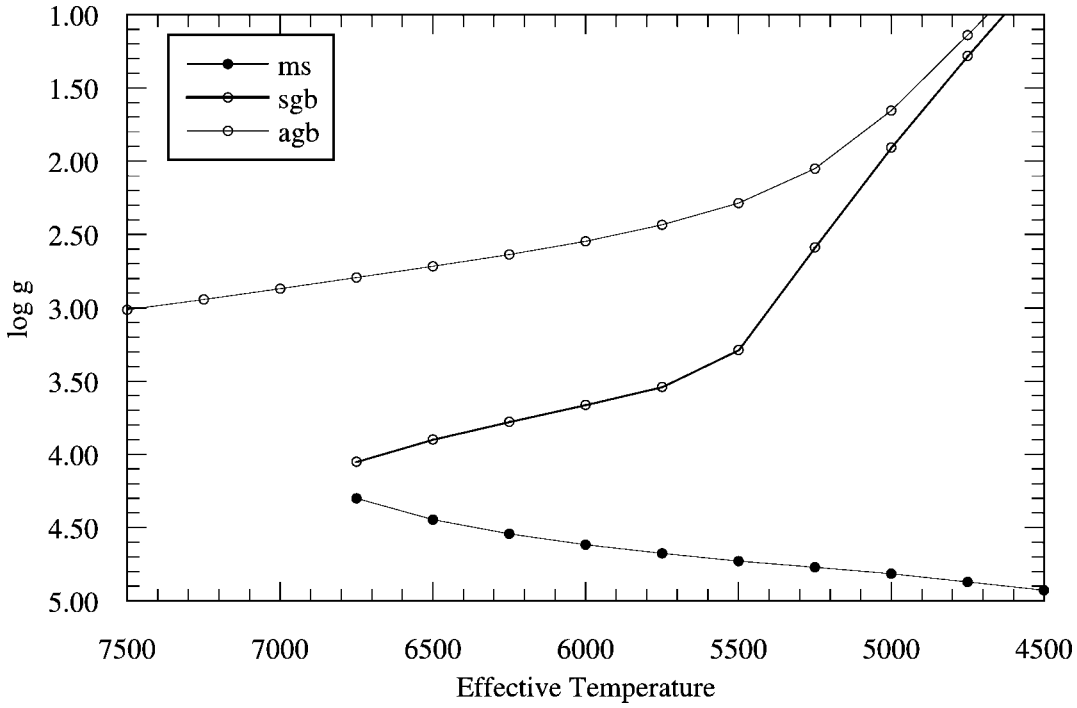

FIG. 1.—Isochrone from Pietrinferni et al. (2006) for 12 Gyr. [*See the electronic edition of PASP for a color version of this figure.*]

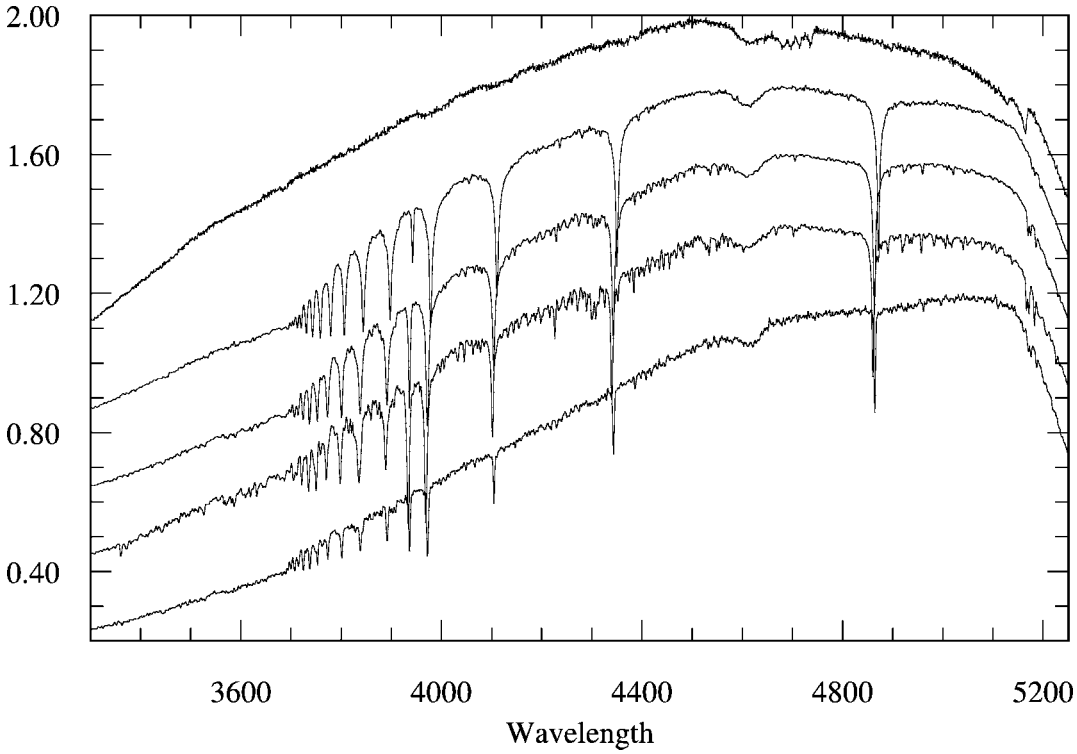

FIG. 2.—Raw extracted blue 2.3 m spectra. See text for details.

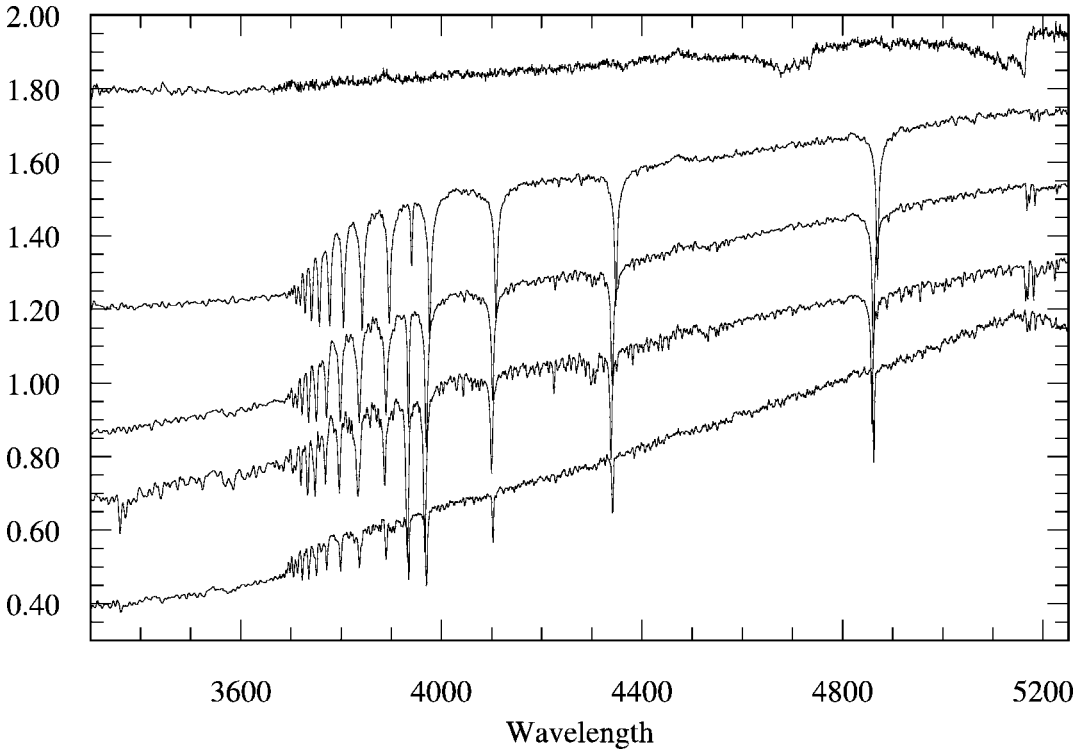

FIG. 3.—Same stars as in Fig. 2, but divided by EG 131.

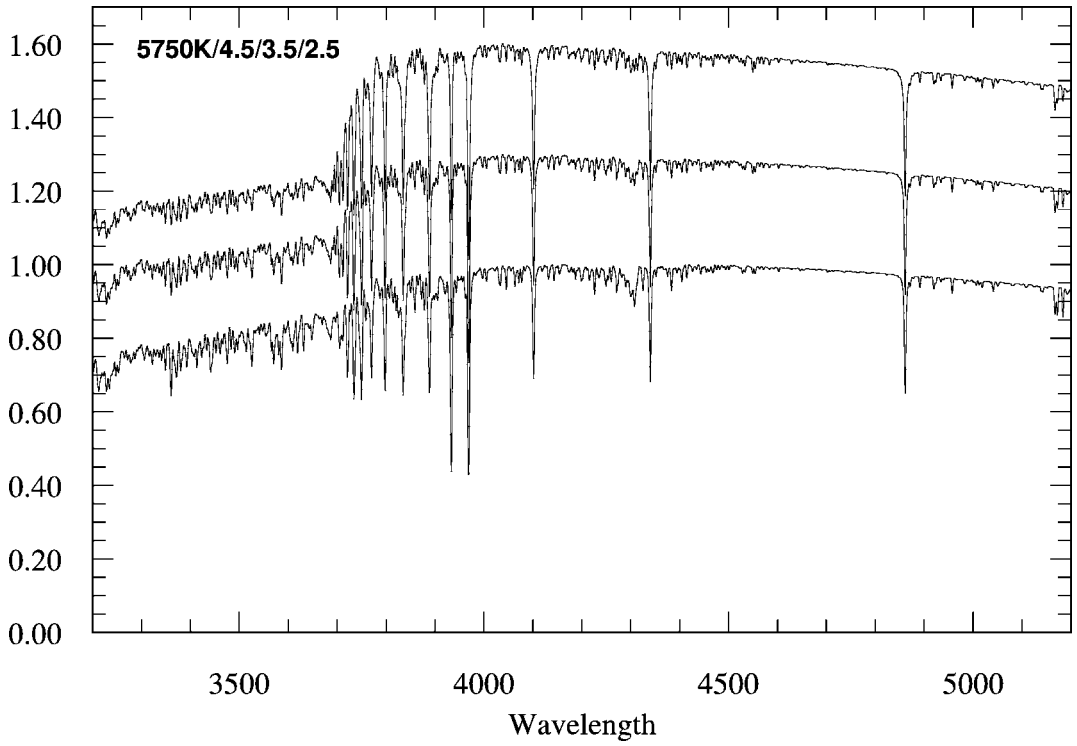

FIG. 4.—Synthetic f_λ spectra for [Fe/H] = −2.5, 5750 K, and $\log g$ = 4.5, 3.5, 2.5.

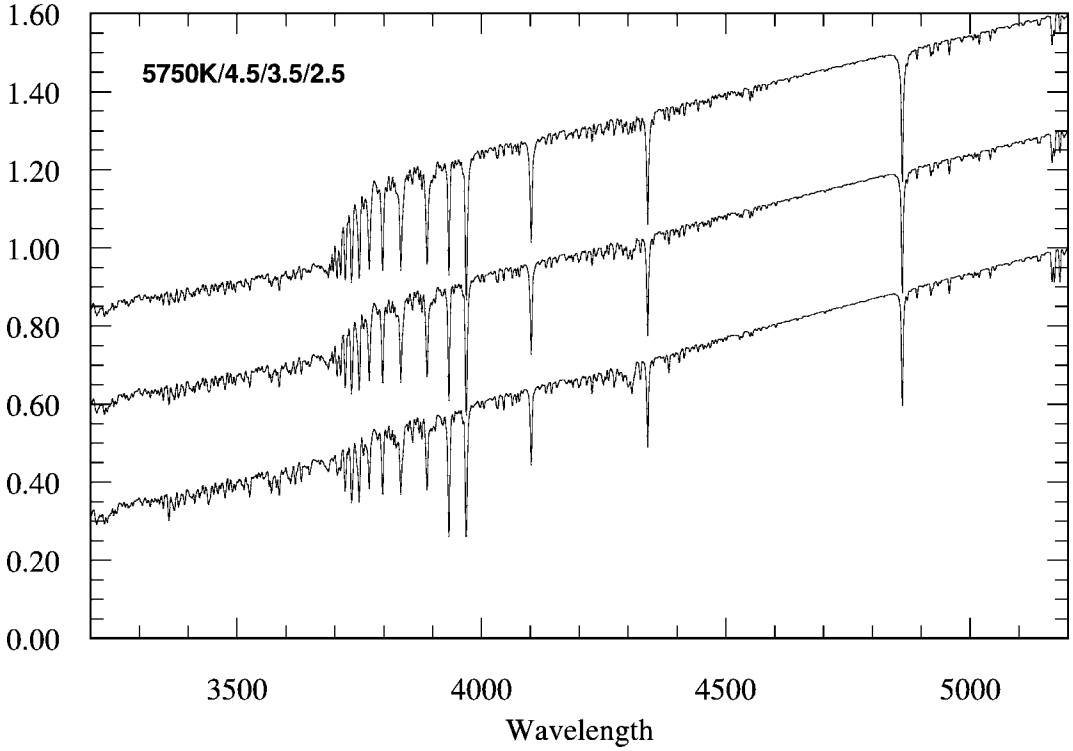

FIG. 5.—Synthetic spectra divided by an 11,800 K BB for [Fe/H] = −2.5, 5750 K, and $\log g = 4.5, 3.5, 2$.

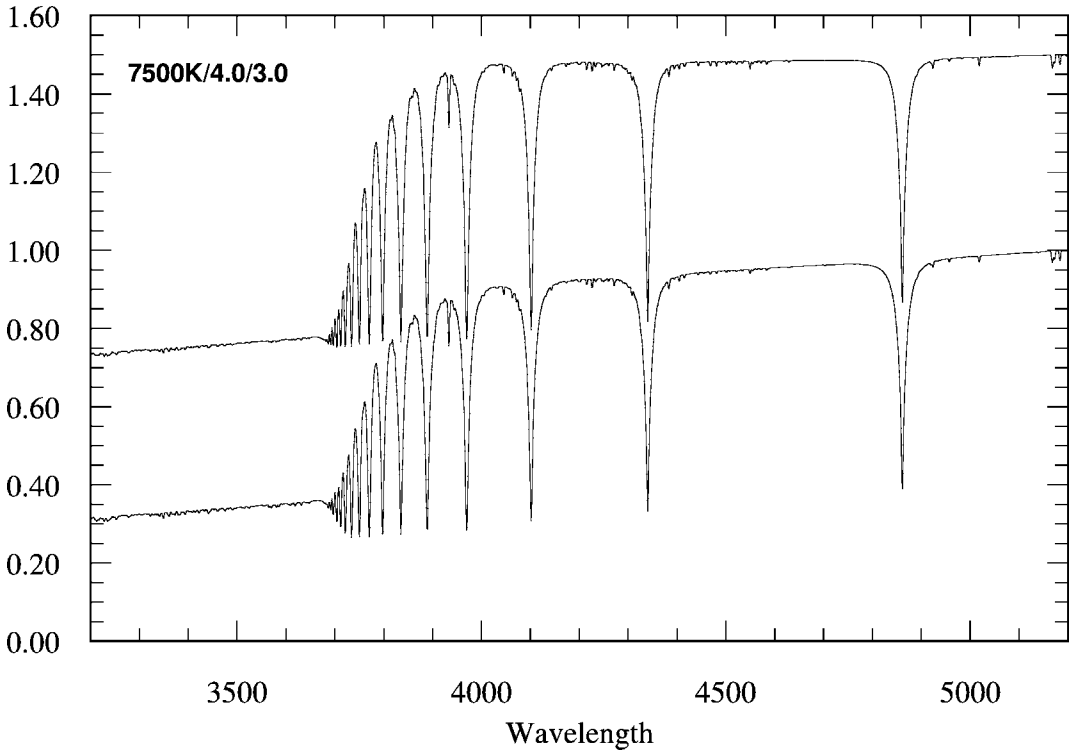

FIG. 6.—Synthetic spectra divided by an 11,800 K BB for [Fe/H] = −2.5, 7500 K, and $\log g = 4.0, 3.0$.

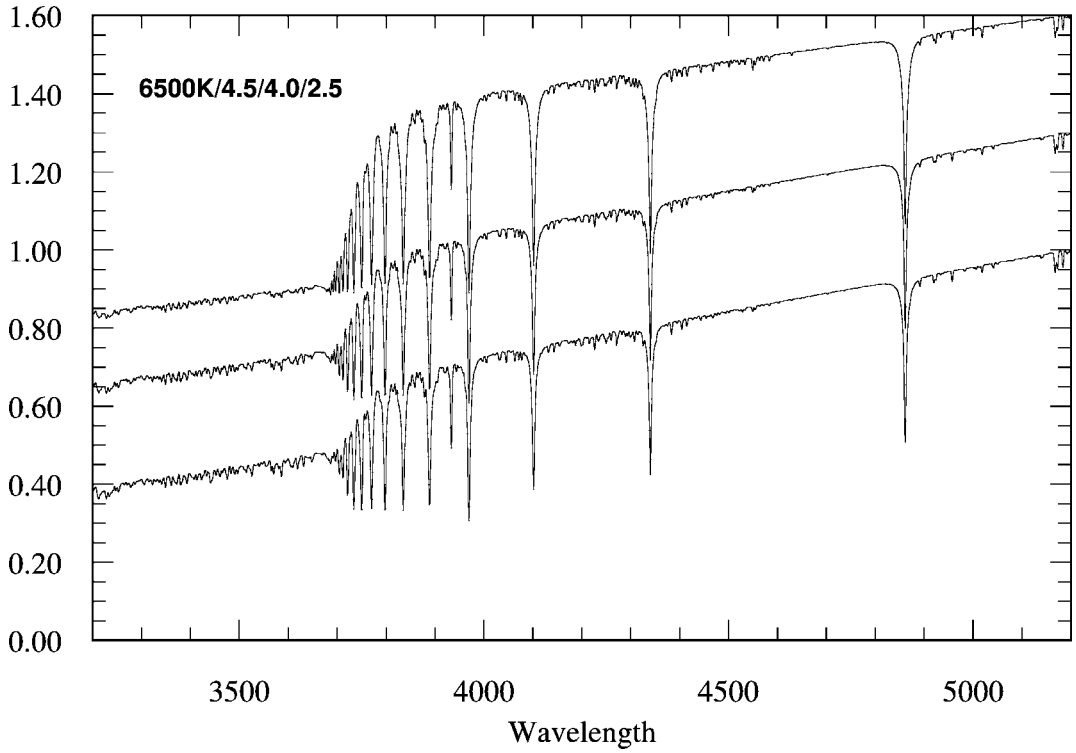

FIG. 7.—Synthetic spectra divided by an 11,800 K BB for [Fe/H] = −2.5, 6500 K, and log g = 4.5, 4.0, 2.5.

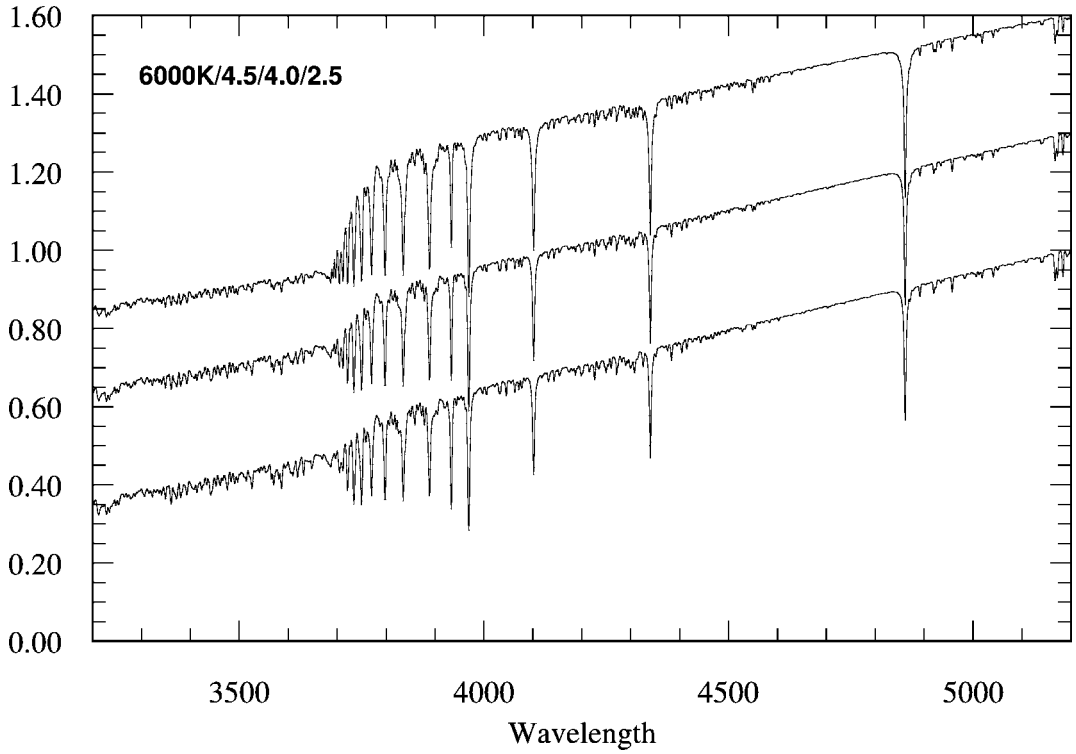

FIG. 8.—Synthetic spectra divided by an 11,800 K BB for [Fe/H] = −2.5, 6000 K, and log g = 4.5, 4.0, 2.5.

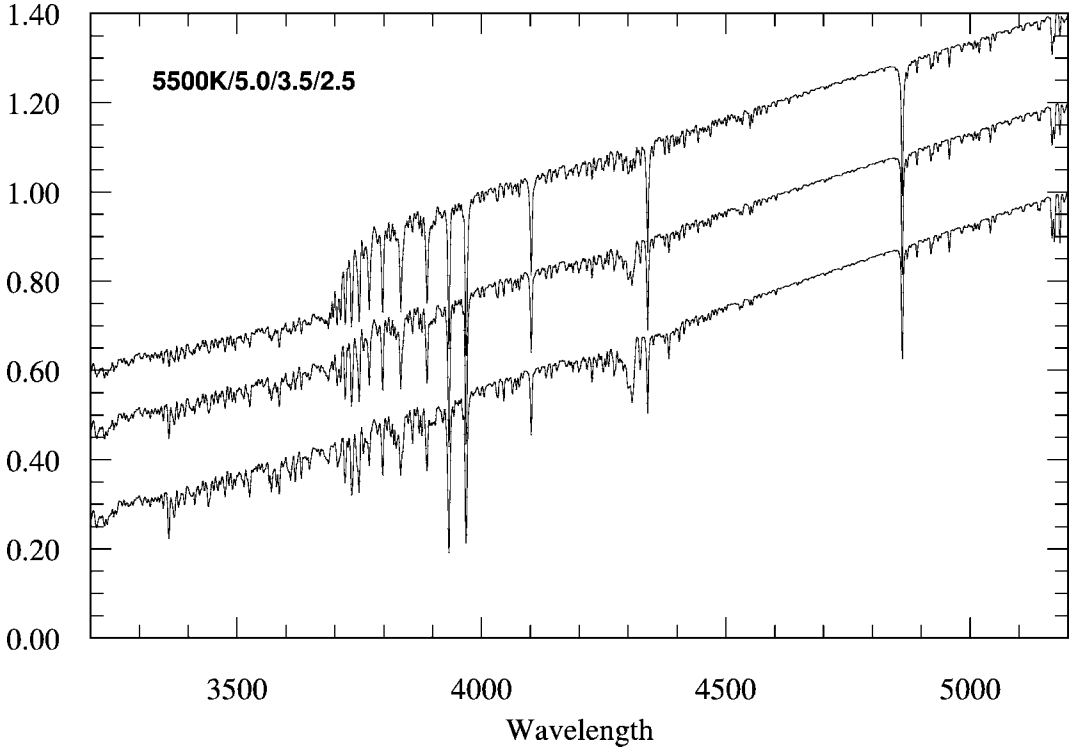

FIG. 9.—Synthetic spectra divided by an 11,800 K BB for [Fe/H] = −2.5, 5500 K, and log g = 5.0, 3.5, 2.0.

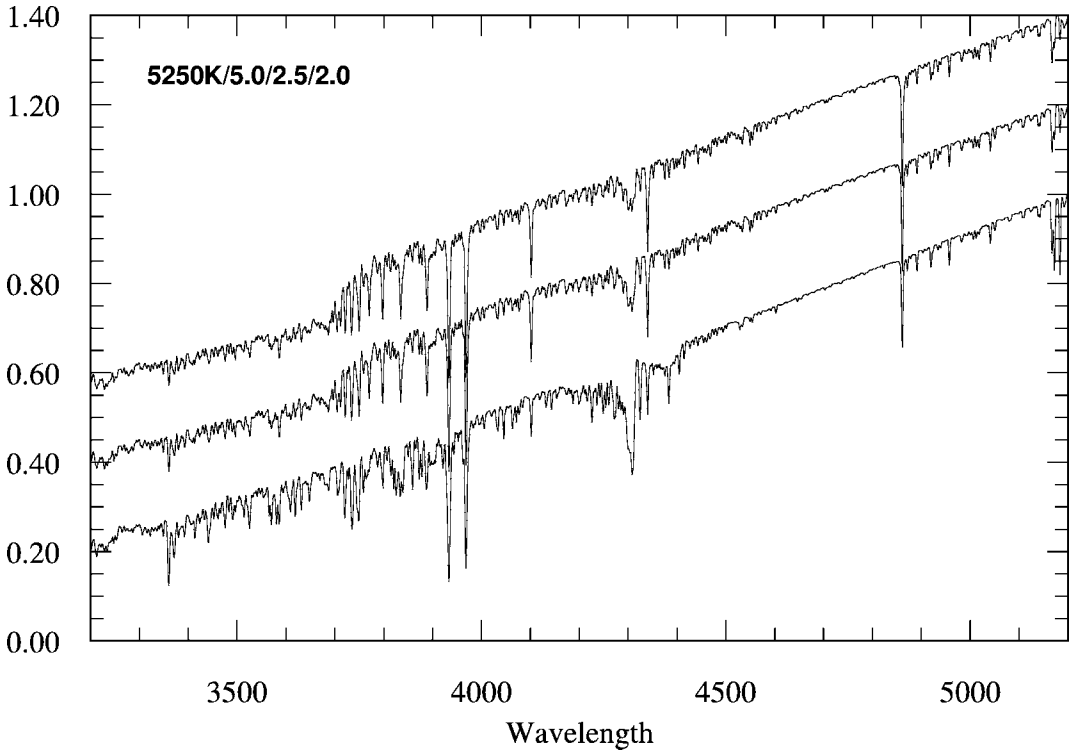

FIG. 10.—Synthetic spectra divided by an 11,800 K BB for [Fe/H] = −2.5, 5250 K, and log g = 5.0, 2.5, 2.0.

TABLE 1
MUNARI ET AL. SPECTRA

		[Fe/H] = −1			[Fe/H] = −1.5			[Fe/H] = −2.5		
$T_{\rm eff}$	log g	BJ	$b-y$	$V-I$	BJ	$b-y$	$V-I$	BJ	$b-y$	$V-I$
6500	4.5	0.40	0.289	0.545	0.36	0.293	0.551	0.31	0.300	0.556
	4.0	0.52	0.279	0.532	0.48	0.283	0.538	0.44	0.290	0.543
	3.5	0.67	0.269	0.519	0.63	0.272	0.523	0.59	0.278	0.528
6250	4.5	0.30	0.319	0.600	0.28	0.323	0.605	0.23	0.330	0.611
	4.0	0.41	0.311	0.591	0.39	0.314	0.597	0.34	0.321	0.602
	3.5	0.52	0.303	0.580	0.51	0.306	0.585	0.46	0.311	0.590
6000	4.5	0.23	0.349	0.656	0.18	0.354	0.662	0.17	0.362	0.668
	4.0	0.31	0.344	0.650	0.28	0.347	0.656	0.24	0.354	0.661
	3.5	0.42	0.338	0.643	0.39	0.340	0.647	0.33	0.346	0.652
5750	4.5	0.16	0.381	0.716	0.13	0.387	0.722	0.09	0.397	0.729
	4.0	0.23	0.377	0.712	0.20	0.381	0.717	0.14	0.389	0.722
	3.5	0.31	0.373	0.706	0.28	0.375	0.711	0.22	0.382	0.716
5500	4.5	0.11	0.413	0.778	0.09	0.422	0.786	0.03	0.437	0.796
	4.0	0.16	0.412	0.776	0.13	0.417	0.781	0.07	0.427	0.788
	3.5	0.23	0.410	0.772	0.18	0.414	0.778	0.12	0.420	0.783
5250	4.5	0.07	0.447	0.848	0.07	0.459	0.856	0.00	0.482	0.872
	3.0	0.20	0.450	0.842	0.16	0.453	0.848	0.11	0.458	0.853

smoothed to approximate the observed medium-resolution spectra. The Munari et al. spectra were smoothed to a resolution of 5 Å, and the MARCS fluxes to 6 Å. All model spectra were divided by an 11,800 K blackbody and then plotted, and the Balmer jumps were measured by hand as for the observed spectra. The size of the Balmer jump in magnitudes are given in Tables 1 and 2. The depth of the Hδ line was also measured, as it is a good temperature indicator; but for comparison with observations, it is necessary to carefully match the resolution, whereas the Balmer jump measurement is not as sensitive to the resolution. The theoretical $b-y, B-V, V-R$, and $V-I$ colors were also computed for the synthetic spectra.

Figure 11 is a plot of the measured Balmer jumps for the Munari et al. spectra ([Fe/H] = −2.5 [*plus sign*] and −1.5 [*square with plus sign*]) and the MARCS spectra ([Fe/H] = −2.5 [*filled circle*] and −1.5 [*open circle*]). There is good general agreement for the two grids, except for the coolest and strongest line spectra, where as noted above, the MARCS sampled photospheric fluxes are not likely to give a good representation of the integrated flux in a limited wavelength region. Full-spectrum synthesis is needed for the MARCS models in order to properly compare them. However, both sets of theoretical spectra show that for temperatures above 5500 K, the Balmer jump can readily distinguish main-sequence and subgiant branch stars, while for temperatures at around 5000 and 5250 K, only gravities below log g = 3.0 can be distinquished

TABLE 2
MARCS STATISTICAL LINE OPACITY SPECTRA

		[Fe/H] = −1			[Fe/H] = −1.5			[Fe/H] = −2.5		
$T_{\rm eff}$	log g	BJ	$b-y$	$V-I$	BJ	$b-y$	$V-I$	BJ	$b-y$	$V-I$
6500	4.5	0.40	0.285	0.540	0.39	0.290	0.546	0.33	0.297	0.553
	4.0	0.55	0.277	0.528	0.50	0.281	0.535	0.47	0.287	0.541
	3.5	0.67	0.267	0.515	0.64	0.270	0.520	0.61	0.277	0.525
6250	4.5	0.33	0.313	0.595	0.30	0.318	0.601	0.26	0.326	0.607
	4.0	0.43	0.307	0.587	0.40	0.312	0.593	0.34	0.318	0.599
	3.5	0.54	0.300	0.576	0.51	0.303	0.582	0.47	0.309	0.587
6000	4.5	0.30	0.342	0.651	0.22	0.349	0.657	0.16	0.357	0.664
	4.0	0.36	0.339	0.646	0.30	0.343	0.652	0.24	0.350	0.657
	3.5	0.42	0.334	0.639	0.39	0.337	0.644	0.34	0.344	0.649
5750	4.5	0.24	0.371	0.711	0.19	0.379	0.716	0.10	0.392	0.724
	4.0	0.28	0.371	0.706	0.23	0.376	0.712	0.15	0.385	0.718
	3.5	0.34	0.368	0.703	0.30	0.372	0.708	0.24	0.378	0.713
5500	4.5	0.24	0.403	0.776	0.15	0.412	0.780	0.06	0.429	0.789
	4.0	0.27	0.403	0.772	0.15	0.409	0.777	0.09	0.422	0.784
	3.5	0.30	0.403	0.770	0.20	0.408	0.774	0.13	0.416	0.780
5250	4.5	0.22	0.437	0.850	0.11	0.445	0.852	0.00	0.472	0.864
	3.5	0.22	0.441	0.842	0.09	0.444	0.845	0.06	0.458	0.853

TABLE 3
BALMER JUMPS MEASURED FROM STIS SPECTRA

Star	[Fe/H]	M_V	BJ	$b-y$	$V-I$	$V-R$
BD 09 2860		4.31	0.39	0.413	0.798	0.393
BD 17 4708	−1.7	4.09	0.39	0.316	0.629	0.306
BD 29 2091	−2.1	5.38	0.16	0.372	0.731	0.352
BD 37 1458	−1.6	2.73	0.20	0.409	0.774	0.373
BD 41 3931	−1.8	6.05	0.08	0.415	0.809	0.401
BD 42 3607	−2.0	5.51	0.19	0.344	0.639	0.308
BD 51 1696	−1.4	5.58	0.19	0.394	0.778	0.380
BD 59 2723	−1.7	5.22	0.33	0.337	0.708	0.340
BD 72 0094	−1.6	3.99	0.40	0.303	0.671	0.315
BD −12 2669	−1.5	4.04	0.65	0.227	0.500	0.236
CD −30 18140	−2.2	4.26	0.42	0.298	0.570	0.270
G115−58	−1.4	3.62	0.37	0.325	0.696	0.335
G029−023	−2.0	2.78	0.39	0.338	0.684	0.334
G88−27	−1.9	−0.82	0.36	0.316	0.654	0.312
HD 002665	−2.0	4.34	0.11	0.537	1.005	0.494
HD 002857	−1.6	1.24	1.38	0.085	0.216	0.089
HD 006755	−1.6	2.16	0.15	0.489	0.957	0.467
HD 016031	−1.8	4.46	0.37	0.305	0.629	0.298
HD 019445	−2.0	5.10	0.27	0.329	0.681	0.319
HD 044007	−1.7	1.62	0.09	0.548	1.045	0.511
HD 045282	−1.5	2.33	0.17	0.448	0.861	0.422
HD 063791	−1.7	−0.89	0.00	0.588	1.127	0.549
HD 087140	−1.6	2.18	0.21	0.461	0.946	0.452
HD 094028	−1.3	4.63	0.30	0.327	0.685	0.324
HD 111721	−1.1	0.56	0.13	0.507	0.981	0.480
HD 128279	−2.1	1.90	0.18	0.449	0.908	0.432
HD 132475	−1.3	3.73	0.28	0.363	0.778	0.365
HD 134439	−1.5	6.74	0.04	0.424	0.857	0.429
HD 134440	−1.5	7.08	0.02	0.516	1.059	0.538
HD 163346		0.30	0.99	0.380	0.839	0.403
HD 163810	−1.4	5.00	0.20	0.384	0.745	0.368
HD 165195	−2.2	4.02		0.894	1.533	0.774
HD 184266	−1.8	0.17	0.55	0.418	0.817	0.400
HD 284248	−1.4	4.77	0.36	0.321	0.659	0.316
HD 345957	−1.3	3.75	0.33	0.345	0.742	0.347

TABLE 4
BALMER JUMPS MEASURED FROM MILES SPECTRA

Star	[Fe/H]	$T_{\rm eff}$	log g	BJ	$b-y$	$B-V$
HD 002665	−2.0	5013	2.35	0.22	0.509	0.720
HD 002796	−2.3	4950	1.36	0.28	0.520	0.724
HD 019445	−2.1	5920	4.40	0.26	0.345	0.445
HD 045282	−1.4	5350	3.20	0.22	0.458	0.658
HD 046703	−1.6	6000	0.40	1.20	0.302	0.421
HD 064090	−1.8	5450	4.45	0.08	0.424	0.608
HD 074000	−2.0	6170	4.20	0.37	0.322	0.407
HD 084937	−2.2	6230	4.00	0.45	0.301	0.374
HD 085773	−2.2	4460	1.00	0.00	0.737	1.046
HD 088609	−2.6	4513	1.30		0.676	0.941
HD 094028	−1.5	5950	4.20	0.31	0.347	0.462
HD 103095	−1.4	5030	4.60	0.09	0.487	0.754
HD 122563	−2.6	4570	1.12	0.09	0.653	0.903
HD 140283	−2.5	5690	3.60	0.30	0.361	0.474
HD 165195	−2.2	4470	1.10		0.830	1.219
HD 187111	−1.8	4260	0.60		0.809	1.215
HD 188510	−1.6	5490	4.70	0.23	0.403	0.591
HD 218502	−1.8	6030	3.80	0.43	0.309	0.414
HD 218857	−1.9	5080	2.40	0.18	0.492	0.705
HD 219617	−1.4	5880	4.00	0.26	0.348	0.478
HD 221170	−2.1	4470	1.00		0.712	1.049
HD 237846	−2.6	4960	1.80	0.20	0.489	0.668
HD 251611	−1.7	5350	3.80	0.15	0.474	0.664
HD 284248	−1.6	6025	4.20	0.39	0.328	0.422

from log $g = 4.5$ main-sequence stars. Cooler than 5000 K, the Balmer jump is virtually impossible to measure, except in the most extreme metal-poor stars.

The model spectra show that the measured Balmer jump increases as the metallicity increases, probably due to the greater strength of metal line–blanketing in the UV than in the blue.

4.2. Observations

There are several excellent spectral libraries that can be used for Balmer jump measurements and comparison with the models. The best library is probably the Next Generation Spectral Library[2] of STIS data, by Gregg (2006). Preliminary versions of the spectra have kindly been provided by M. Gregg and J. M. Appelaniz. The Sanchez-Blanquez et al. (2006) library[3] is of similar quality and resolution, but has shorter wavelength coverage (3500–7500 Å).

[2] See http://lifshitz.ucdavis.edu/~mgregg/gregg/ngsl/download.html.
[3] See the MILES library, http://www.ucm.es/info/Astrof/miles/miles.html.

Table 3 lists the measured Balmer jumps of the STIS spectra, together with the *Hipparcos* M_V and colors computed from the spectra. Table 4 lists the measured Balmer jumps of the MILES (Medium-resolution INT Library of Empirical Spectra) spectra, together with the atmospheric parameters from Cenarro et al. (2007) and the $b-y$ and $B-V$ colors computed from the spectra.

In Figure 12, the M_V versus $b-y$ diagram for the STIS spectra is shown, together with a halo isochrone. Some of the M_V values are poorly determined because of large uncertainties in the parallax, and there are at least four stars whose absolute magnitudes are in disagreement with their Balmer jump measurements shown in Figure 13.

Figure 13 is a plot of the observed Balmer jumps for the STIS sample versus $b-y$. Lines have been drawn through the main-sequence, subgiant, and giant branch stars, as indicated from Figure 12. The stars whose M_V values differ significantly from their Balmer jumps are marked in Figure 12. The theoretical values for the Munari et al. [Fe/H] $= -1.5$ and -2.5 spectra are also shown for log $g = 3.5$, 4.0, and 4.5, and temperatures $T_{\rm eff} = 6500$, 6250, 6000, 5750, 5500, and 5250 K. The Balmer jumps from the synthetic spectra are in good agreement with the observed loci of metal-poor stars. Precise derivation of the gravities of individual stars involves knowledge of the metallicity and temperature (and the reddening, if fluxes are used), which is beyond the scope of this paper.

5. SUMMARY

Dividing extracted raw spectra by the spectrum of a warm near-blackbody object such as EG 131, L745−46a, LHS 43,

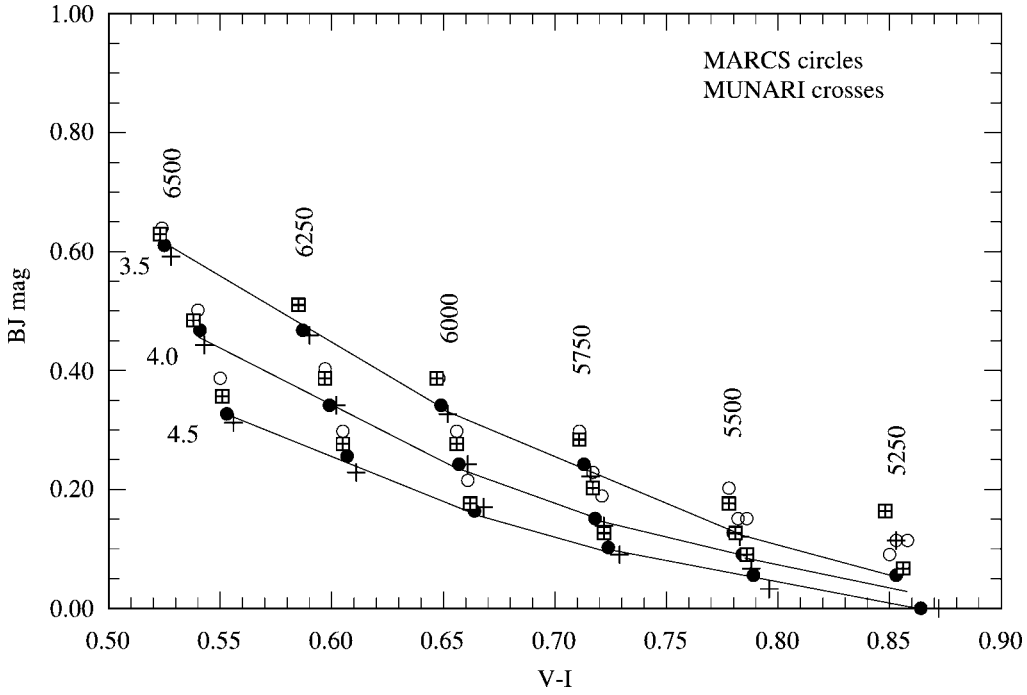

FIG. 11.—Measured Balmer jumps vs. $V-I$ color for model spectra for [Fe/H] $=-1.5$ and -2.5. Connecting lines are drawn through points for the same gravity for the [Fe/H] $=-2.5$ spectra.

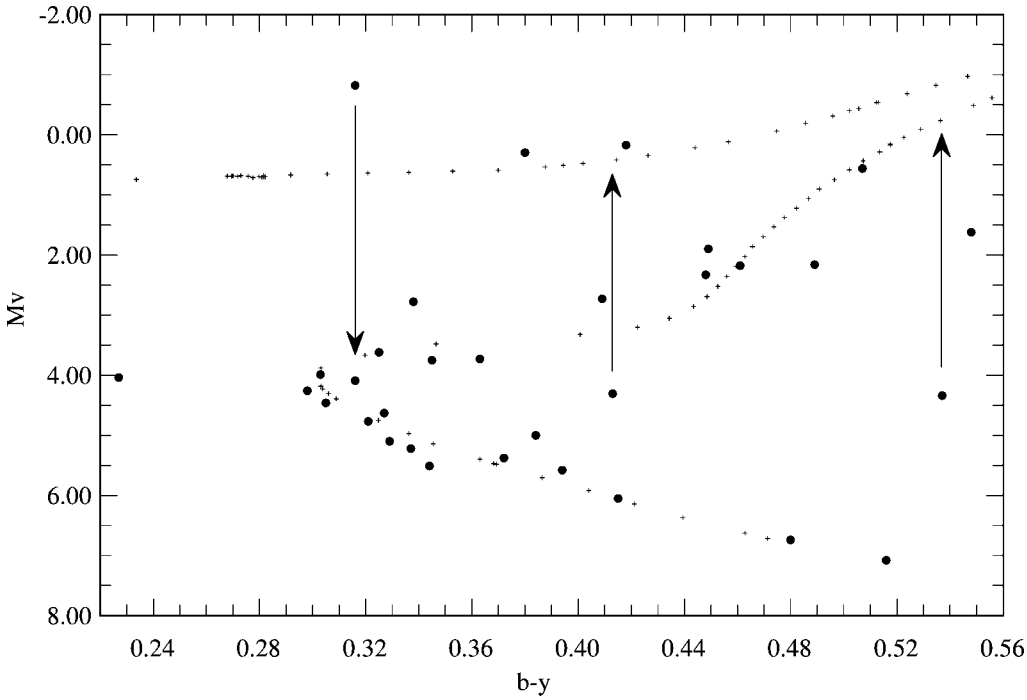

FIG. 12.—Absolute magnitude M_V vs. $b-y$ diagram for the selection of STIS spectra of low-metallicity stars listed in Table 3. A halo isochrone is shown for orientation. The lines with arrows indicate the appropriate shifts for those stars whose M_V values are inconsistent with their measured Balmer jumps.

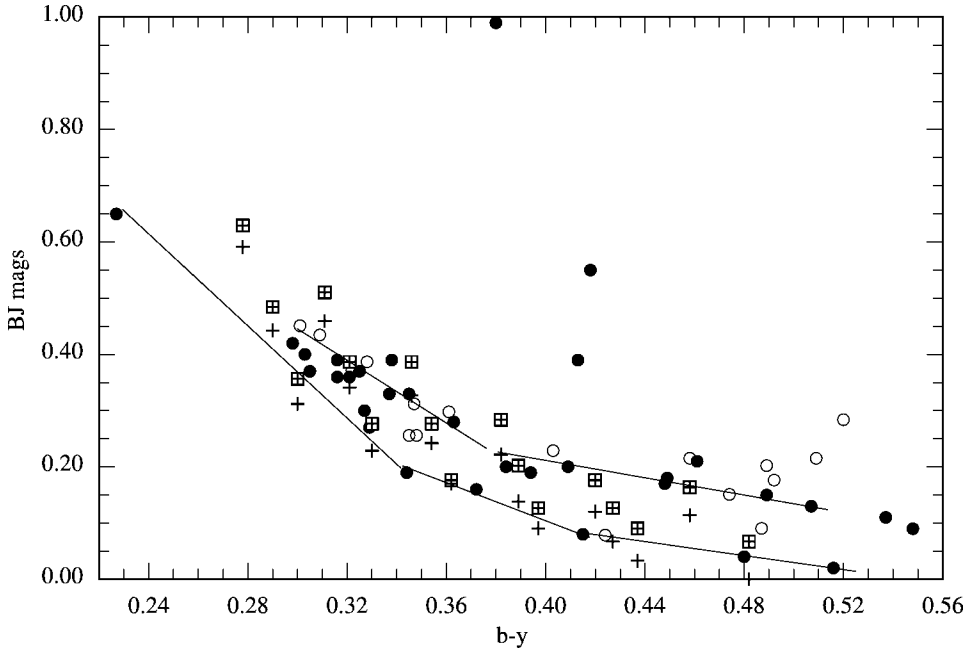

FIG. 13.—Measured Balmer jumps vs. $b - y$ color for the STIS stars (*filled circles*) and MILES spectra (*open circles*). Lines have been drawn to connect the stars on the main sequence and the subgiant and giant branch as identified in Fig. 12. The same relation for the Munari et al. spectra for [Fe/H] $= -1.5$ plotted in Fig. 11 is also shown.

or LHS 4043 results in spectra whose continua above and below the Balmer discontinuity are close to straight lines, thus making it easy to measure the size of the Balmer jump accurately.

The recommendation is to observe a warm near-blackbody star at least once per run for each grating setting used, then divide all extracted raw spectra by a template made from the normalized extracted blackbody spectrum by removing any obvious lines or bands it may have, or by fitting the continuum. In order to accurately measure the theoretical Balmer jumps from synthetic spectra such as those of Munari et al. (2005), it is also important to divide the synthetic spectra by the normalized theoretical blackbody spectrum of a blackbody temperature similar to the template star used.

Having followed these recommendations and measured the Balmer jump, the effective gravity can be derived from the model spectra. If the effective temperature of the FGK star is known to within 100 K, the Balmer jump will yield an effective gravity to about 0.2 dex for the hotter stars and 0.5 dex for the cooler stars, sufficient precision to determine whether the star is a main-sequence, giant branch, or horizontal/asymptotic giant branch star.

Best spectrophotometric results are achieved if an atmospheric dispersion corrector is used or if the spectrograph is rotated to put the parallactic angle along the slit. This is not essential to measure the monochromatic Balmer jump, but it does ensure that the spectra can be accurately calibrated onto a relative absolute flux scale, and that other temperature-sensitive colors can be derived.

I am grateful to Dr. Lajos Balazs, Director of Konkoly Observatory, and Dr. Katalin Olah for their hospitality during the writing of this paper. I am also grateful to Dr. Fiorella Castelli for providing the synthetic spectra, to Dr. Santi Cassisi for computing additional isochrones, and to Drs. Michael Gregg and Jesus Maiz Appelaniz for the preliminary NGSL STIS spectra.

REFERENCES

Bergeron, P., Leggett, S. K., & Ruiz, M. T. 2001, ApJS, 133, 413
Bessell, M. S. 1999, PASP, 111, 1426
Cenarro, A. J., et al. 2007, MNRAS, 374, 664
Dufour, P., Bergeron, P., & Fontaine, G. 2005, ApJ, 627, 404
Filippenko, A. V. 1982, PASP, 94, 715
Greenstein, J. L., & Liebert, J. W. 1990, ApJ, 360, 662
Gregg, M. D., et al. 2006, in 2005 *HST* Calibration Workshop, *Hubble* after the Transition to Two-Gyro Mode, ed. A. M. Koekemoer, P. Goudfrooij, & L. L. Dressel (Greenbelt: GSFC), 209
Koester, D., & Wolff, B. A&A, 357, 587
Munari, U., Sordo, R., Castelli, F., & Zwitter, T. 2005, A&A, 442, 1127
Pietrinferni, A., Cassisi, S., Salaris, M., & Castelli, F. 2006, ApJ, 642, 797
Salasnich, B., Girardi, L., Weiss, A., & Chiosi, C. 2000, A&A, 361, 1023
Sanchez-Blazquez, P., et al. 2006, MNRAS, 371, 708
VandenBerg, D. A. 2000, ApJS, 129, 315